Engineering Geology 180 (2014) 130–144

Contents lists available at ScienceDirect

Engineering Geology

journal homepage: www.elsevier.com/locate/enggeo

Temporary strong-motion observation network for Wenchuan aftershocks and site classification

Ruizhi Wen [a,*], Yefei Ren [a], Zhenghua Zhou [b], Xiaojun Li [c]

[a] Key Laboratory of Earthquake Engineering and Engineering Vibration, Institute of Engineering Mechanics, China Earthquake Administration, Harbin 150080, China
[b] College of Transportation Science & Engineering, Nanjing University of Technology, Nanjing 211816, China
[c] Institute of Geophysics, China Earthquake Administration, Beijing 100081, China

ARTICLE INFO

Article history:
Accepted 10 May 2014
Available online 17 May 2014

Keywords:
Wenchuan earthquake
Temporary observation
Strong-motion record
Site classification

ABSTRACT

The $M_s = 8.0$ ($M_W = 7.9$) Wenchuan earthquake of May 12, 2008 was the largest destructive event on the Chinese mainland since the 1976 Tangshan earthquake. Thousands of aftershocks occurred in the following months. To improve the performance of the National Strong-Motion Observation Network System (NSMONS) in China, a temporary strong-motion observation network was quickly set up along the Longmenshan Fault in the most heavily damaged areas. We briefly reviewed the history and the advances in temporary strong-motion observation in China where temporary networks have been proven to be a very effective way of accumulating strong-motion records from large aftershocks. Then the case of the Wenchuan earthquake was described together with the process of compiling, standardizing and disseminating the collected data. A total of 3250 records were collected from 92 temporary stations for 949 aftershocks between May 13 and October 10, 2008. The largest peak ground acceleration (PGA) is 966.5 cm/s^2 from an $M_S = 4.2$ earthquake on August 10, 2008. Some general statistics, such as the number of recorded events with various magnitudes, PGA and epicentral distance, were analyzed and compared with the data from permanent stations. These results show that the temporary network can effectively compensate for the large instrument spacing of the permanent network to record near-field ground motion. Since no borehole data are available for those temporary stations, their site classifications are inferred using a horizontal-to-vertical spectral ratio (HVSR) technique based on the observed strong-motion records. A scheme of six site classes is proposed to improve the reliability of the HVSR technique. As a result, the site classes of 66 temporary stations are recommended finally.

1. Introduction

Strong-motion seismology is generally concerned with the measurement, interpretation and estimation of the strong ground shaking generated by potentially damaging earthquakes. Observation of strong-ground motion is more difficult than those in other fields of seismology due to the infrequency of large earthquakes and the lack of the appropriate instrumentation in the area of strong ground shaking. Chinese strong-motion observation network has made considerable progress since the first permanent station commenced its operation in 1962. By 2001 there were a total of 488 permanent strong-motion stations on Chinese mainland (Gao et al., 2001). In 2008, as part of the national 10th Five-Year Plan, the National Strong-Motion Observation Network System (NSMONS) was established, funded by the Chinese central government. This new-generation network is comprised of 1154 permanent free-field stations shown in Fig. 1, 12 special observation arrays, 200 temporary instruments and a network management system (Li et al., 2008). However, the network cannot possibly monitor all seismic areas in China because of large instrument spacing in a range of 50 km to hundreds of kilometers. The use of temporary strong-motion observation network is an important and cost-effective approach to enhance the ability of near-field monitoring.

Temporary strong-motion observation has been deployed extensively in China and has been proven to be effective in recording strong ground motion due to their advantages of real-time and portability. Real-time, of course, is valuable because the observation team can be sent to the scene at the first indications of a moderate or large earthquake—the earlier, the better. The flexibility of instrument installation contributes to its portability, and temporary observation points could be adjusted depending on variations of the aftershock locations.

* Corresponding author. Tel.: +86 451 86652617; fax: +86 451 86664755.
E-mail addresses: ruizhi@iem.net.cn (R. Wen), renyefei@iem.net.cn (Y. Ren), bjsmoc@163.com (Z. Zhou), beerli@vip.sina.com (X. Li).

http://dx.doi.org/10.1016/j.enggeo.2014.05.001
0013-7952/

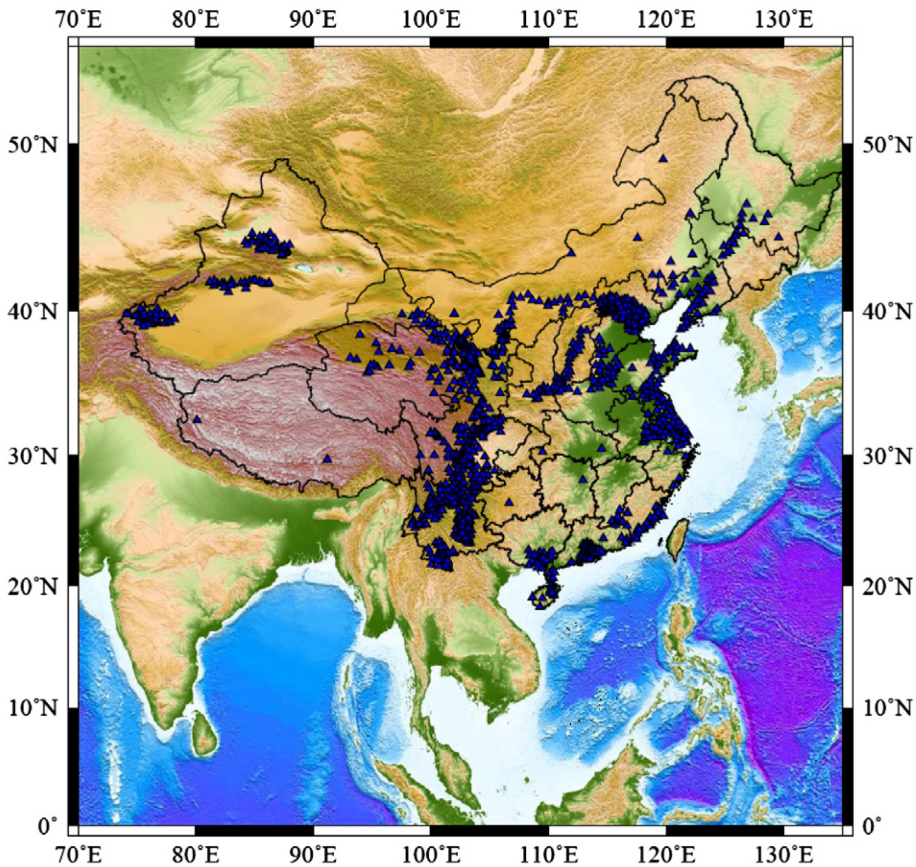

Fig. 1. National Strong-Motion Observation Network System (permanent free-field stations).

China Earthquake Administration (CEA) responded quickly to the news of the Wenchuan earthquake on May 12, 2008 by dispatching a temporary strong-motion observation team to monitor the aftershocks (Wen et al., 2009). We coordinated and participated in this work. The observation processes and obtained strong-motion records were introduced in this article. In addition, as a required parameter for strong-motion stations, the site classes of the temporary stations were classified by four empirical HVSR methods.

2. Temporary strong-motion observation in China

Recording strong ground motion in China was initiated in 1956 by Professor Liu Huixian, the pioneer of earthquake engineering in China. A strong-motion research team was organized by the Institute of Engineering Mechanics, China Earthquake Administration (IEM/CEA) in the winter of 1960. In March 8, 1966, the $M_S = 6.8$ Xingtai earthquake occurred, followed by the $M_S = 7.2$ earthquake on March 22. A team was immediately sent to the damaged area to perform the observation of a large number of aftershocks. Since then, the temporary observation program has been recognized as an effective way of monitoring strong-motion events in China, and has provided most of strong-motion records on the Chinese mainland prior to 2007 (Gao et al., 2001; Li et al., 2008). An obvious limitation of a post-event temporary strong-motion network is the usual missing chance to record the ground motion from the main shock. However, following short-term and imminent earthquake predictions, temporary observation networks have in fact captured the main shock records in some cases, including the Songpan earthquake on August 16, 1976 (Gao et al., 2001) and the Shidian earthquake on April 12, 2001 (Zhao et al., 2001).

Between 1966 and 1976, temporary strong-motion observation programs in China played a much more important role in recording strong motions than the sparse network of permanent stations in China. Table 1 lists the typical observation programs for 1966–1976, with the $M_S = 7.8$ Great Tangshan earthquake observations being the most successful case. When the Tangshan event occurred on July 28, 1976, there were no permanent strong-motion stations around the meizoseismal area, and five temporary stations were set up to record the near-field ground motion generated by the large aftershocks. Fig. 2 shows that the permanent stations located around Beijing and were far from the aftershock epicenters. Five temporary analog accelerographs were triggered more than 200 times by 134 aftershocks of magnitude $M_L \geq 3$ until October 1, 1976. A total of 163 records were released finally. The

Table 1
Temporary strong-motion observation programs (1966–1976).

Date	Earthquake name	Magnitude
March 8 and 22, 1966	Xingtai	M_s6.8 and M_s7.2
Oct. 2, 1966	Changchun	M_s5.2
March 27, 1967	Hejian	M_s6.7
July 18, 1969	Bohai Region	M_s7.4
July 26, 1969	Yangjiang	M_s6.4
Jan. 5, 1970	Tonghai	M_s7.8
March 23 and 24,1971	Wuqia	M_s6.0 and M_s6.1
Feb. 4, 1975	Haicheng	M_s7.3
May 29, 1976	Longling	M_s7.3 and M_s7.4
July 28, 1967	Tangshan	M_s7.8
Aug. 16, 1976	Songpan	M_s7.2

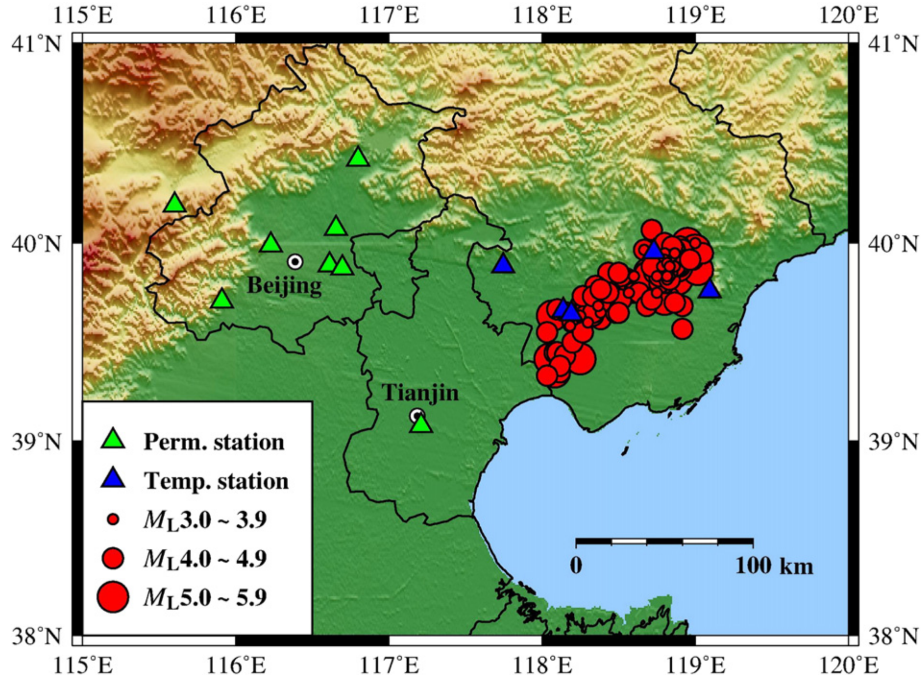

Fig. 2. Temporary strong-motion observation in Great Tangshan earthquake.

maximum peak ground acceleration of 159 cm/s^2 was recorded at the Qian'an station and this record is still commonly used today as the ground-motion input for structural analyses in China. In terms of the number of records and acceleration amplitudes, this operation was a milestone in the history of temporary strong-motion observations during the analog instrument era in China (Liu, 1986).

Now, as one of the sub-projects of NSMONS, the Temporary Strong-Motion Program (TSMP) has gradually developed to its

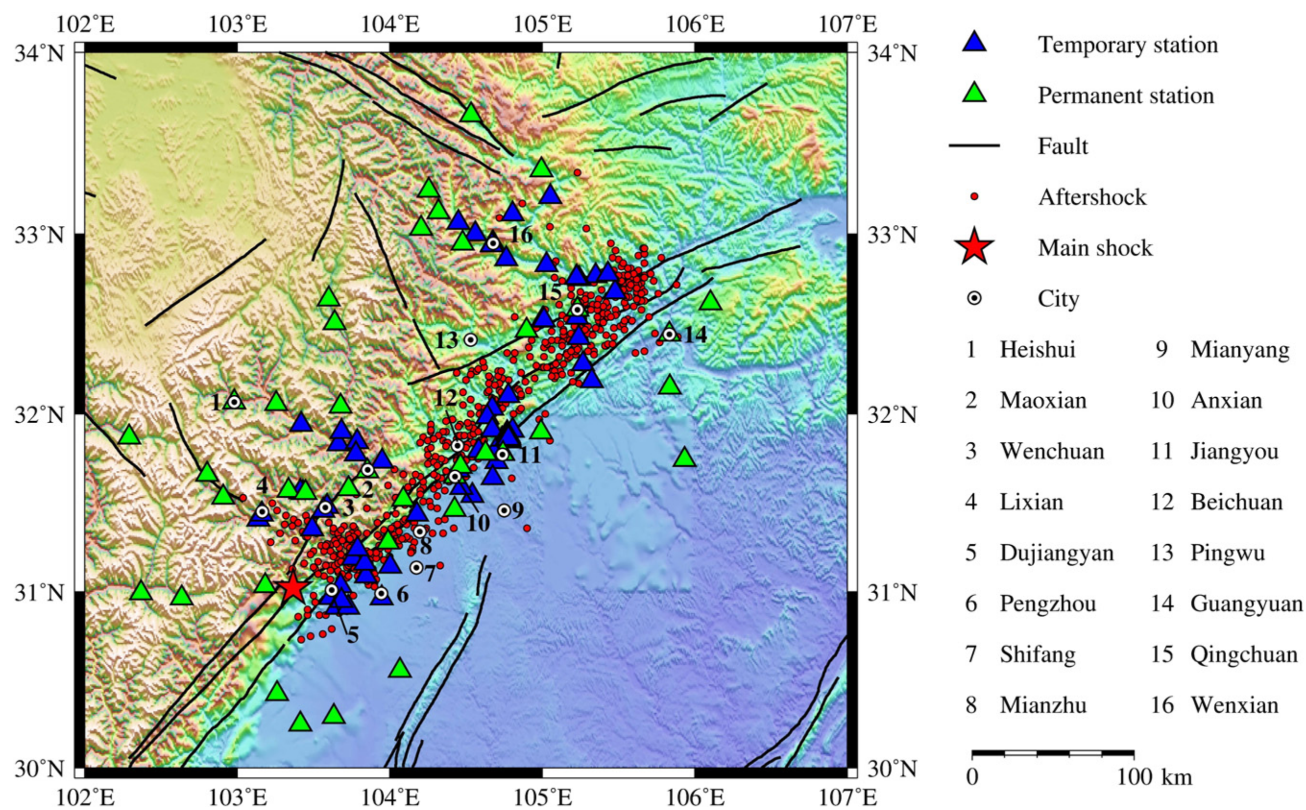

Fig. 3. Temporary and permanent strong-motion networks for Wenchuan earthquake.

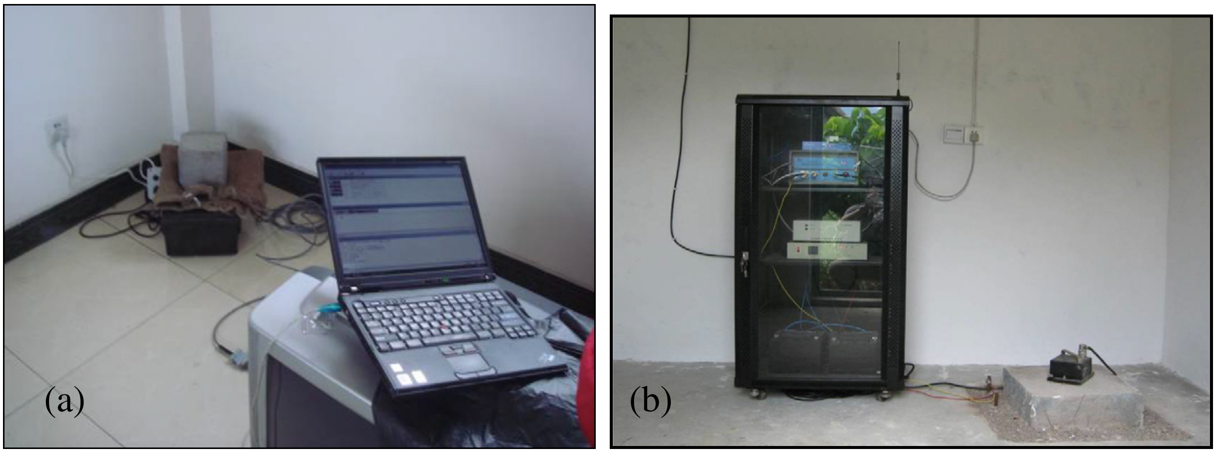

Fig. 4. Typical observation arrangement for a temporary station (a) and a permanent station (b).

maturity in China, with 200 sets of high-quality instruments. TSMP is responsible for four sub-regions in Chinese mainland, with four regional centers: Beijing, Lanzhou, Nanjing and Kunming. China Strong-Motion Networks Center (CSMNC) is located near Beijing suburbs with 80 sets of accelerographs, and the storages of remaining 120 sets are in the other three centers. CSMNC is responsible for record retrieval, processing and dissemination, technical support and housing the instrument maintenance and calibration.

3. Temporary strong-motion observation during Wenchuan earthquake

The 2008 Wenchuan earthquake occurred along the Longmenshan fault, and the surrounding area is the most earthquake-prone region in western China. Since, as mentioned, the station spacing of the permanent strong-motion network of NSMONS are too large to record the near-field ground motion, the temporary strong-motion network began to be installed in selected areas just 24 h after the main shock.

3.1. Observation background

To obtain as many near-field strong ground-motion records as possible, most of the instruments were installed in areas where few permanent strong-motion stations were located. On the footwall side of the fault, the instruments were installed along a line parallel to the fault strike, that is, from Dujiangyan to Pengzhou, Shifang, Mianzhu, Mianyang, Jiangyou and Guangyuan. On the hanging wall side, the instruments were installed along three transverse lines sub-perpendicular to the fault from Wenchuan to Lixian, from Heishui to Maoxian, and from Wenxian to Qingchuan. A total of 92 temporary stations were eventually installed. The information including station code, name, location, site condition and number of records is presented in Appendix A. Fig. 3 shows the location of all temporary and permanent stations associated with the 2008 Wenchuan earthquake sequence. As the trend of the aftershock

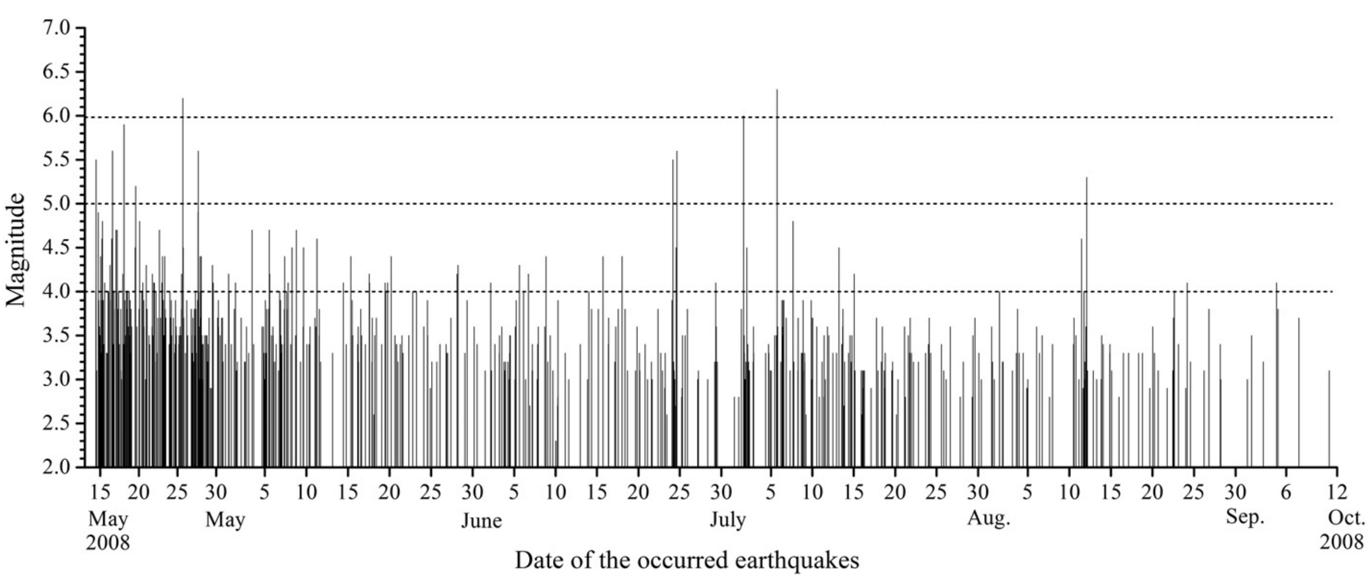

Fig. 5. Magnitude-date sequence released officially by CENC for the earthquakes from which the strong-motion records used in the present study.

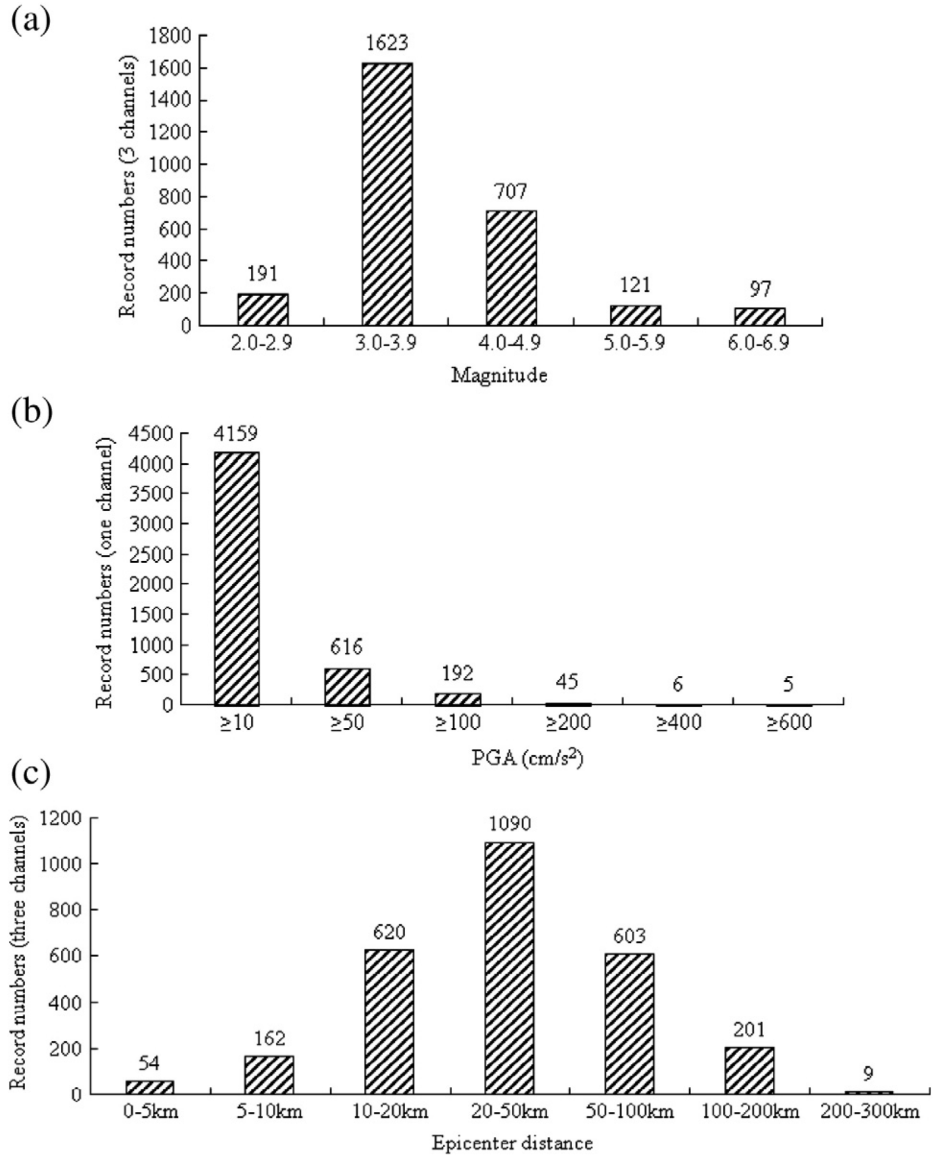

Fig. 6. Record numbers versus magnitude, PGA and epicenter distance.

epicenters moved from South–West to North–East, the observation sites were gradually adjusted. The relocation of temporary stations were mainly distributed in the areas around Wenchuan, Dujiangyan and Lixian during May and June; Maoxian, Beichuan, Jiangyou and Anxian during July and August; and Qingchuan and Pingwu during August, September and October in 2008.

Site selection is difficult for the temporary stations because of the serious damage caused by the main shock. The main problem was

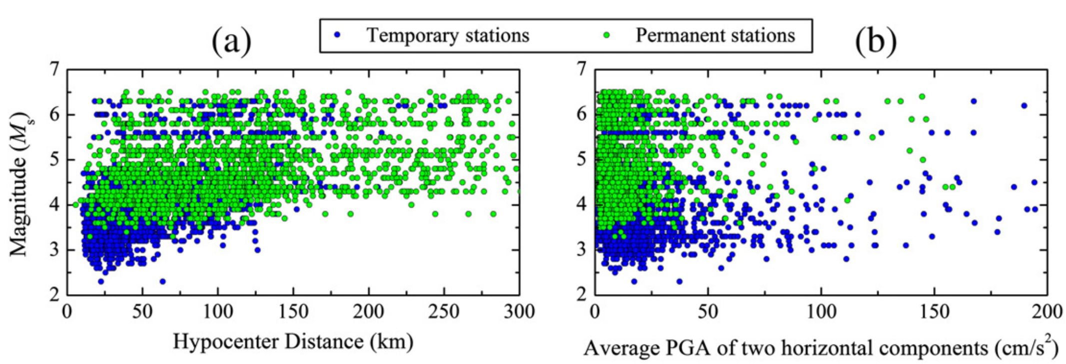

Fig. 7. Comparison of the magnitude and (a) hypocenter distance and (b) PGA as measured by the temporary and permanent networks.

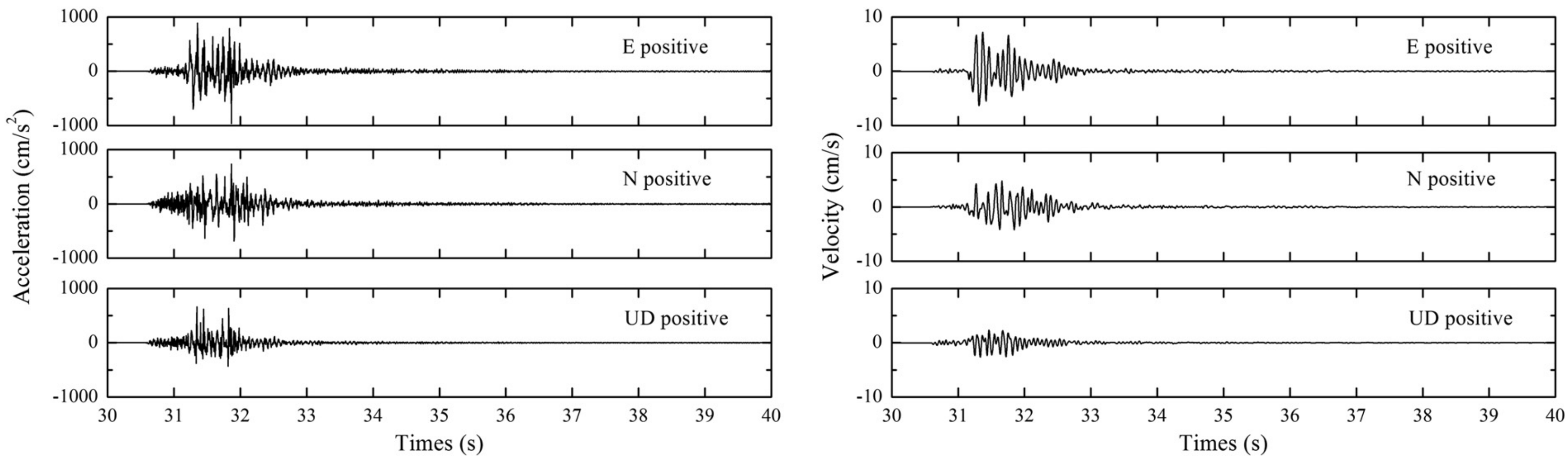

Fig. 8. Acceleration and velocity time-histories of L0027 associated with the maximum PGA obtained in Wenchuan aftershocks (PGA in EW, NS, UD component is -966.5 cm/s^2, 734.3 cm/s^2 and 658.9 cm/s^2, and PGV is 7.17 cm/s, 4.77 cm/s, -2.63 cm/s respectively).

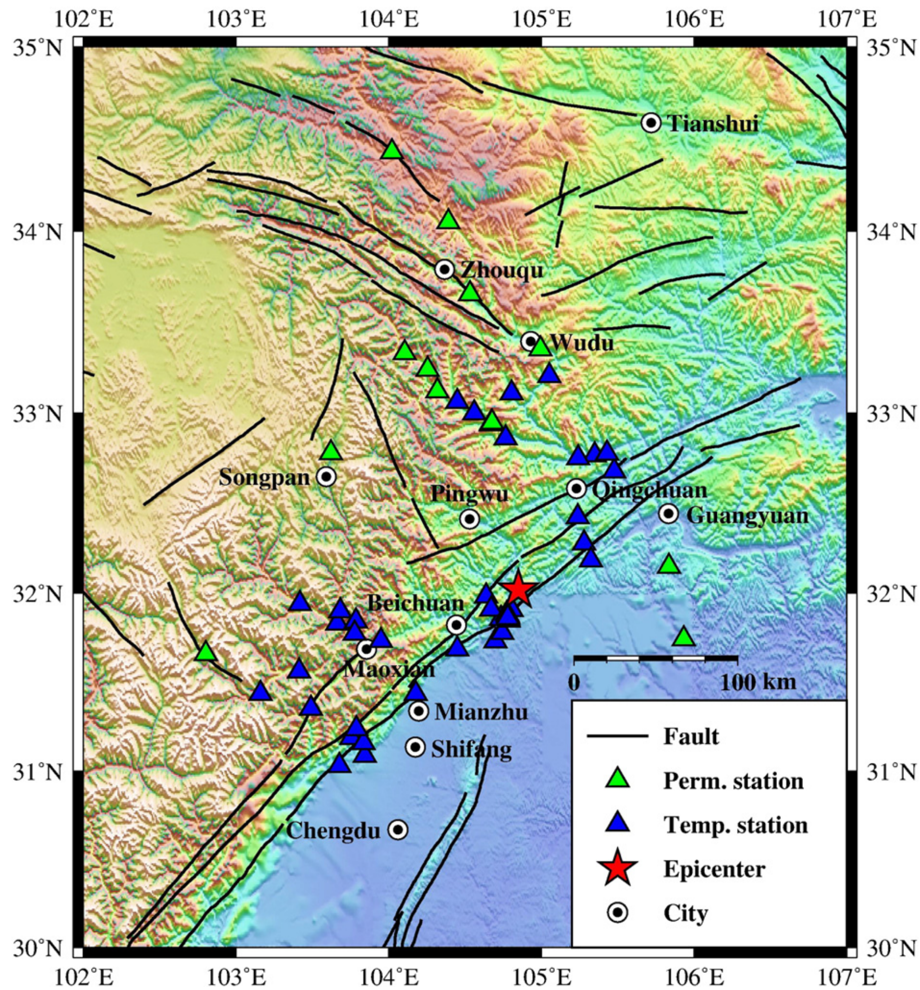

Fig. 9. The triggered strong-motion stations in $M_S = 6.0$ earthquake occurred on 16:32:41, Aug. 1, 2008 within the epicenter distance of 300 km.

availability of a reliable electricity supply. Fortunately, some temporary power-generating equipment was available in local government buildings or gas stations, and observation instruments were then installed in those public facilities. Most accelerographs were installed on the ground surface of hard soil or bedrock when possible. Instrument installation strictly followed the technology standards to meet the requirements of the relevant code (China Earthquake Administration, 2006). To make sure that the instrument is well fixed, it is either glued down, or by using a heavy object on the top of the instrument box as shown in Fig. 4(a). In permanent stations, an accelerograph is usually secured to a concrete pillar foundation, generally 40 cm × 40 cm. Fig. 4(b) shows a typical instrument installation arrangement for a permanent station.

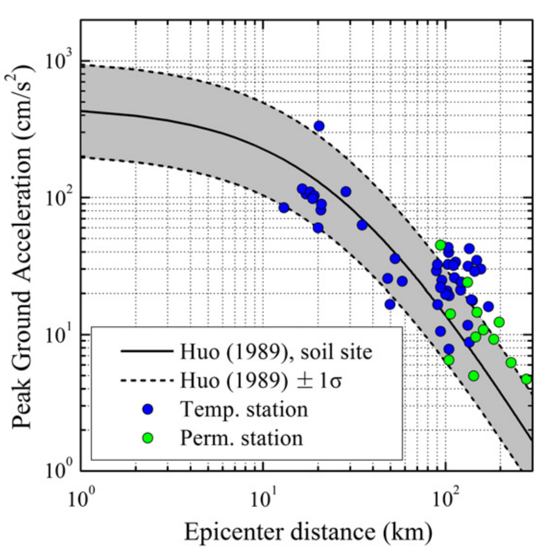

Fig. 10. Comparison of the observed PGAs and the common-used GMPE of China.

Table 2
Site class definition used in Japan earthquake resistant design code (Japan Road Association, 1980) and the approximately corresponding NEHRP site class (Building Seismic Safety Council, BSSC, 2003).

Site classes	Site natural period (s)	Average shear-wave velocity	NEHPR class
SC I: (rock/stiff soil)	$T_G < 0.2$	$V_{30} > 600$ m/s	A + B
SC II: (hard soil)	$0.2 \le T_G < 0.4$	300 m/s < $V_{30} \le 600$ m/s	C
SC III: (medium soil)	$0.4 \le T_G < 0.6$	200 m/s < $V_{30} \le 300$ m/s	D
SC IV: (soft soil)	$T_G \ge 0.6$	$V_{30} \le 200$ m/s	E

Note: T_G: site natural period; V_s30: average shear wave velocity of 30 m surface soil layer

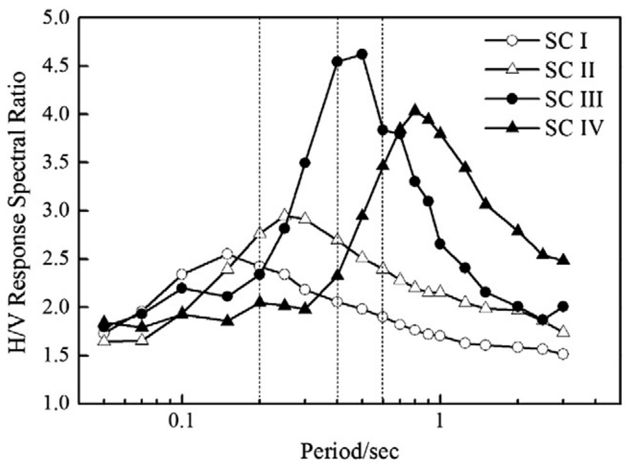

Fig. 11. Mean HVSR plots for different site classes (Zhao et al., 2006). The vertical dashed lines represent the bounds of two adjacent site classes provided in Table 2.

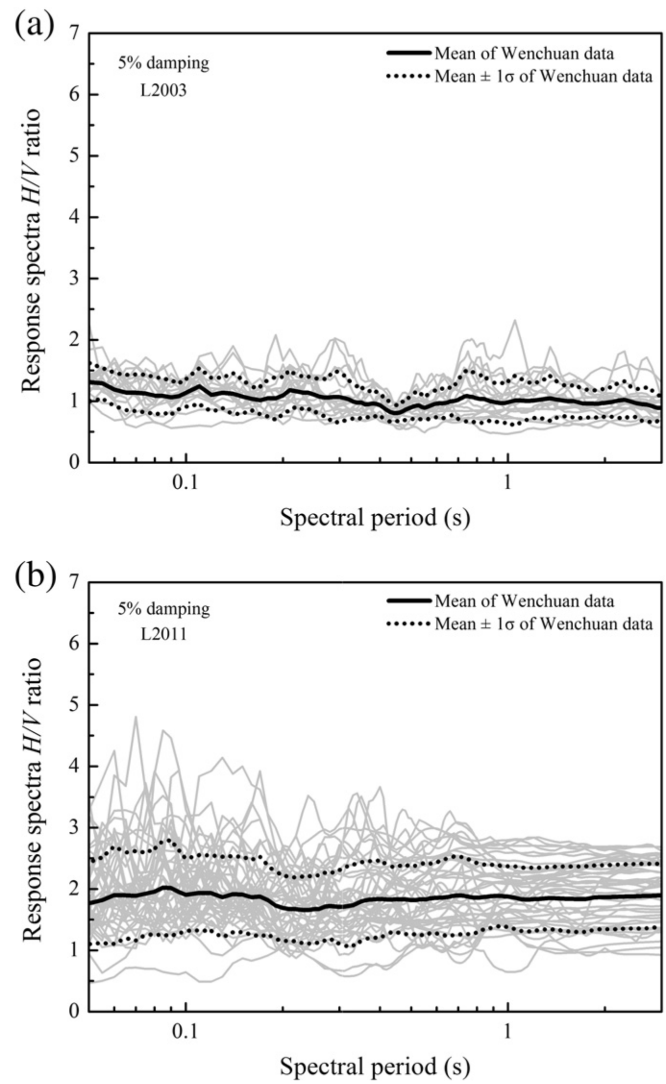

Fig. 12. Typical flat HVSRs without any evident peaks for stations L2003 and L2011. The heavy solid lines indicate the mean HVSR, and the dotted lines indicate the mean HSVR ± one standard deviation. The thin gray lines indicate the HVSR for each record. The left panel shows the HSVR for station L2013 that was proposed as a Class I0 site, because the average HVSR amplitude is close to 1 at all spectral periods. The right panel shows the HSVR for station L2011 that was proposed as a Class I site because the average HVSR amplitude is larger than 1 at all spectral periods.

3.2. Strong-motion records from the temporary stations for the 2008 Wenchuan earthquake aftershocks

From May 13, 2008 to October 10, 2008, a total of 3250 3-channel strong-motion records from 949 aftershock events were gathered. Of these, 2214 were recorded in 600 events described in the official earthquake catalog of the China Earthquake Network Center (CENC); 525 corresponded to the earthquake catalog produced by the regional Sichuan Province Seismic Network in China. However, 437 were not found in any published earthquake catalog, and in 74 cases, the exact record time was automatically reset by the accelerograph due to power outages. That is, a total of 2739 aftershock records were published. The numbers of records for temporary stations are given in Appendix A. Fig. 5 shows the magnitude vs. event date for the 600 aftershocks published by CENC. 3 of these exceeded $M_S = 6.0$, 8 were $M_S = 5.0–5.9$, 95 were $M_S = 4.0–4.9$, 452 were $M_S = 3.0–3.9$ and the remaining 42 were below $M_S = 3.0$. The epicenters of all these aftershocks are mapped in Fig. 3.

Fig. 6 shows the histograms of occurrence frequency for all 2739 records vs. (a) magnitude, (b) peak ground acceleration (PGA), and (c) epicentral distances. Most epicentral distances for these aftershock records were within 100 km, suggesting that there is a very good chance to record near-field ground motions from aftershocks. Most of the records were obtained from aftershocks with a magnitude $M_S = 3.0$ to $M_S = 3.9$ and a PGA from 10 cm/s^2 to 50 cm/s^2. However, 248 sets of time-histories have a PGA greater than 100 cm/s^2, compensating for the lack of large PGA records from the permanent network. Fig. 7 compares the record distribution with respect to magnitude versus hypocenter distance (Fig. 7(a)) and magnitude versus PGA (Fig. 7(b)) obtained from the temporary and permanent networks. The benefit of the temporary observation stations is obvious that many more near-field records with higher PGA from small and moderate aftershocks could be captured by the temporary network than by the permanent network.

Table 3
Criterion of the proposed site classes on the basis of Zhao et al. (2006).

Site class	criterion
I0	Hard rock site, flat H/V ratio (peak is not identifiable), amplitude closes to 1 at all spectral periods
I	Single or multiple peaks, HVSR corresponds to the match of spectral shape of SC I of Zhao et al. (2006); or flat H/V ratio (peak is not identifiable), amplitude is larger than 1 at all spectral periods
II	Single or multiple peaks, HVSR corresponds to the match of spectral shape of SC II of Zhao et al. (2006)
III	Single or multiple peaks, HVSR corresponds to the match of spectral shape of SC III of Zhao et al. (2006)
IV	Single or multiple peaks, HVSR corresponds to the match of spectral shape of SC IV of Zhao et al. (2006)
V	Multiple peaks, HVSR does not appear to match the spectral shape of any classes by Zhao et al. (2006)

3.3. Typical records

The largest PGA was −966.5 cm/s^2 in an east–west (E–W) direction recorded at Huangping Town station (code L0027) in an $M_S = 4.2$ earthquake occurred in 00:31:36, August 10, 2008 (Beijing time) in Qingchuan County. The PGA is even greater than the largest one from

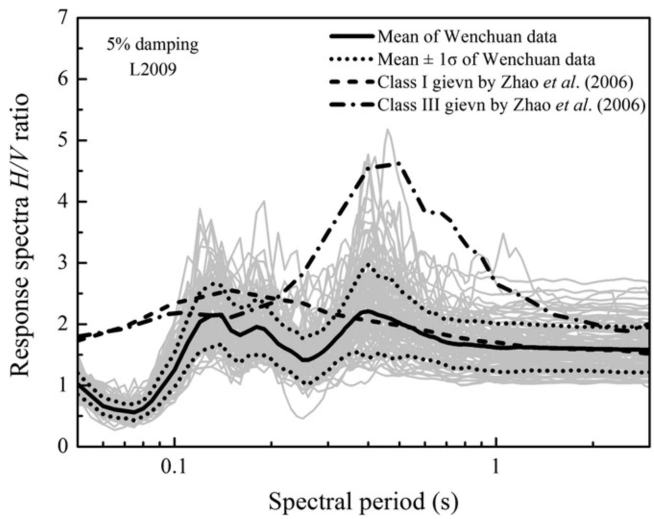

Fig. 13. The HVSR of a typical example for a Class V site from station L2009. Class V was assigned to this site because its HVSR shape does not appear to match either SC I or SC III of Zhao et al. (2006). Thin gray curves indicate the HVSR of each record.

the main shock (957.7 cm/s^2 E–W component) recorded by the permanent Wolong Station (code 51WCW). This level of PGA from this comparatively small earthquake was somewhat surprising. Fig. 8 shows the acceleration and velocity time-histories that suggest a high-frequency ground motion with a large PGA, a short-duration of 1–2 s, and a small peak ground velocity (PGV) in all three components. Inferred from the P-wave and S-wave arrival times, the recording site L0027 may be just directly above the hypocenter of this $M_S = 4.2$ event, and such that the high-frequency contents were recorded before considerable attenuation as the seismic waves propagated through the crust medium.

At 16:32:41 (Beijing time), August 1, 2008, an aftershock of magnitude $M_S = 6.0$ with an epicenter at 104.85°E, 32.02°N occurred near Beichuan County. Fifteen permanent stations and 46 temporary stations were triggered, for which the basic information had been given by Li (2009a, b). Only the temporary stations were near the epicenter region and all the permanent stations were at least 100 km from the epicenter. Fig. 9 shows the epicenter locations and the stations within an epicentral distance of 300 km. Fig. 10 compares the observed PGAs at these stations with the predicted ones by a commonly used Ground Motion Prediction Equations (GMPEs) for southwestern China given by Huo (1989). The observed PGAs within an epicentral distance of 60 km were somewhat smaller than the predicted ones, while many within 100–200 km were considerably higher.

4. Site classifications

Many post-earthquake investigations and experiences show that local site condition has a large effect on ground-motion characteristics and earthquake damage. As an important parameter, site classification of a strong-motion station should be available for developing GMPEs. Since there is no borehole data for the temporary stations, a large number of aftershock records are used to estimate site classes of these stations based on empirical techniques, such as the horizontal-to-vertical spectral ratio (HVSR). This technique was already used for the site classification of the permanent stations in the Wenchuan area (Wen et al., 2010, 2011). In this study, four classification methods were used for those temporary stations.

Table 4
Site classification by different methods.

Station code	T_p (s)	Method 1	Method 2	Method 3	Method 4 ※
L0001	0.17	I	II	II	I
L0002	0.25/0.07	II	I	II	I
L0003	0.31	II	II	II	II
L0004	0.16	I	II	I	I
L0005	0.27	II	II	II	II
L0006	0.37	II	I	II	II
L0007	0.17	I	II	II	I
L0008	0.36	II	II	II	III
L0009	0.22	II	II	II	II
L0010	0.2	II	III	II	II
L0011	0.18	I	II	II	II
L0012	0.2	II	I	I	I
L0013	0.21	II	II	II	II
L0014*	0.43/0.16	III	V	V	V
L0016*	0.53/0.21/0.12	III	V	V	V
L0017	0.52/0.30	III	II	III	III
L0018*	0.37/0.14	II	V	V	V
L0019	0.3	II	I	II	II
L0020	–	I	I	I	I
L0021*	–	I	I0	I0	I0
L0022	0.13	I	I	I	I
L0023	–	I	II	III	I
L0025	0.28	II	II	II	II
L0027	0.08	I	I	IV	I
L0028	0.17/0.07	I	I	I	I
L0041	0.11	I	I	I	I
L0042	0.18	I	I	I	I
L0043	0.35	II	I	III	II
L0044	0.2	II	I	II	II
L0045	0.22	II	I	II	I
L0046	0.24	II	I	II	II
L0047	0.16	I	I	I	I
L0048	0.17	I	II	II	II
L0049	0.19	I	II	II	II
L0050	0.24	II	II	II	II
L0051	0.15	I	I	II	II
L0052	0.13	I	I	II	I
L0053	0.16	I	I	II	I
L0054*	0.21/0.09	II	V	V	V
L0055	0.21	II	II	II	II
L0056	0.09	I	II	I	I
L1001	0.14	I	I	II	I
L1002	0.28/0.09	II	I	III	II
L1004	0.18	I	I	II	I
L2001	0.15	I	I	II	I
L2002*	0.4/0.16	III	V	V	V
L2003*	–	I	I0	I0	I0
L2004	0.28	II	I	III	II
L2005	0.23	II	I	II	II
L2006	–	I	I	III	I
L2007	0.26/0.13	II	I	II	I
L2008	0.35/0.19	II	II	II	II
L2009*	0.4/0.14	III	V	V	V
L2010	–	I	I	III	I
L2011	–	I	I	IV	I
L2012	–	I	I	IV	I
L2015	0.27	II	II	III	II
L2016	0.24	II	I	II	I
L2017	0.34	II	I	III	II
L2018	–	I	I	IV	I
L2019*	–	I	I0	I0	I0
L2020*	0.44/0.12	III	V	V	V
L2022	0.13	I	I	I	I
L2025	0.12	I	II	IV	I
L2026	0.29	II	I	II	II
L2027	0.17	I	II	II	I

Note: T_p, the peak period identified by HVSR.
"*", means that the site is classified as Class I0 or Class V.
"–", means that the site has non-existent peak period.
"/", means that the site has more than one peak period.
"※", recommended classification in this paper.

Table 5
Number of sites in each site class given by different methods.

Site class	Method 1	Method 2	Method 3	Method 4
I0	–	3	3	3
I	32	34	10	30
II	28	21	32	24
III	6	1	9	2
IV	0	0	5	0
V	–	7	7	7

4.1. Classification methods

Method 1: This depends on the natural period of the site, as shown in Table 2, used in Japan earthquake resistant design code (Japan Road Association, 1980).

Method 2: This was proposed by Zhao et al. (2006) who suggested a site classification index SI using mean horizontal-to-vertical (H/V) spectral ratios over a wide range of spectral periods, calculated from:

$$\mathrm{SI}_k = \frac{2}{n}\sum_{i=1}^{n} F(-\mathrm{abs}[\ln(\mu_i) - \ln(\overline{\mu}_{ki})]) \quad (1)$$

where k is the site class number, n is the total number of periods, F is the normal cumulative distribution function, μ_i is the mean H/V ratio for the ith period of a given site, and $\overline{\mu}_{ki}$ is the standard H/V ratio for the ith period with respect to the kth site class, as shown in Fig. 11.

Method 3: This is an update to improve the accuracy of Method 2 by Ghasemi et al. (2009), who redesigned the SI based on Spearman's rank correlation coefficient:

$$\mathrm{SI}_k = 1 - 6\sum_{i=1}^{n} \frac{d_i^2}{n(n^2-1)} \quad (2)$$

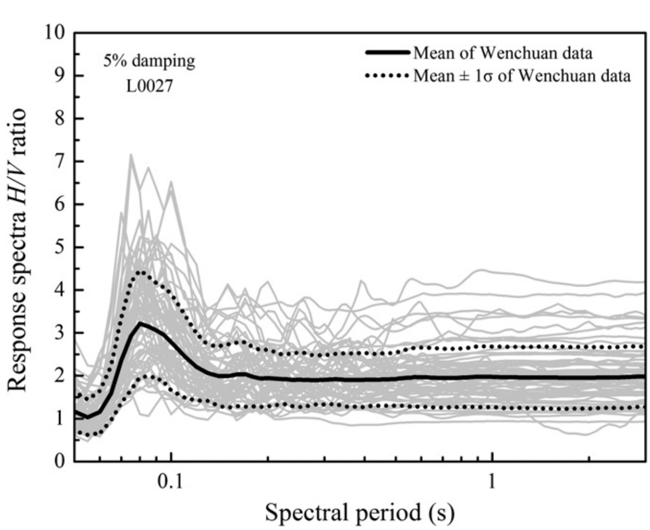

Fig. 14. The HVSR for station L0027. This is an example for sites that have low natural period of around 0.1 s classified as Class I by Methods 1, 2, and 4 but Class IV by Method 3.

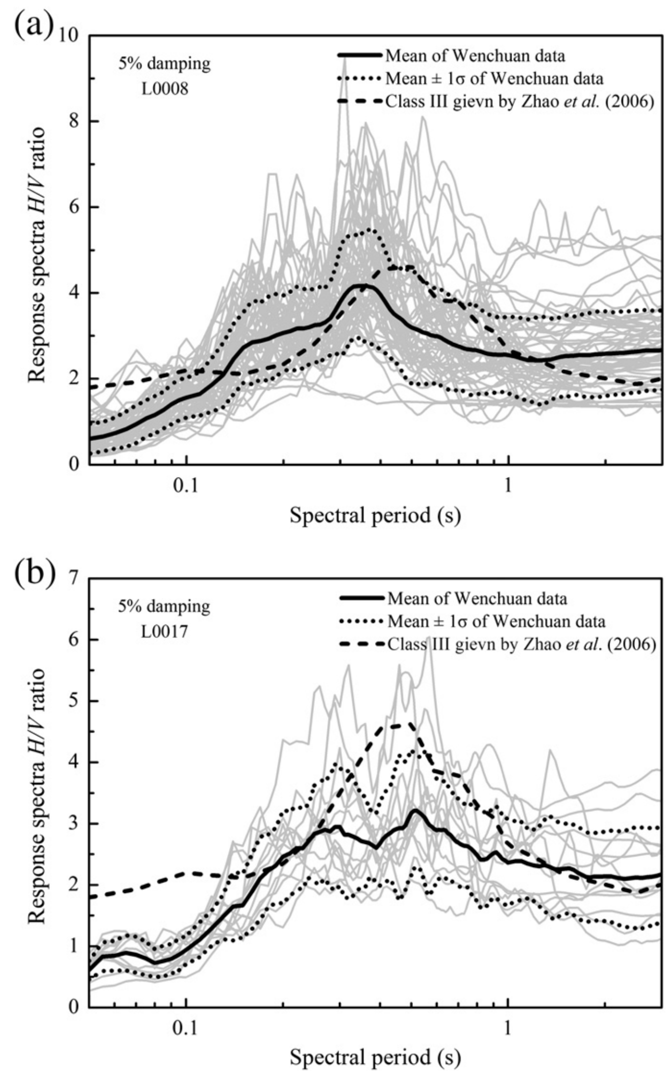

Fig. 15. HVSRs of two stations (a) L0008 and (b) L0017 classifed as Class III.

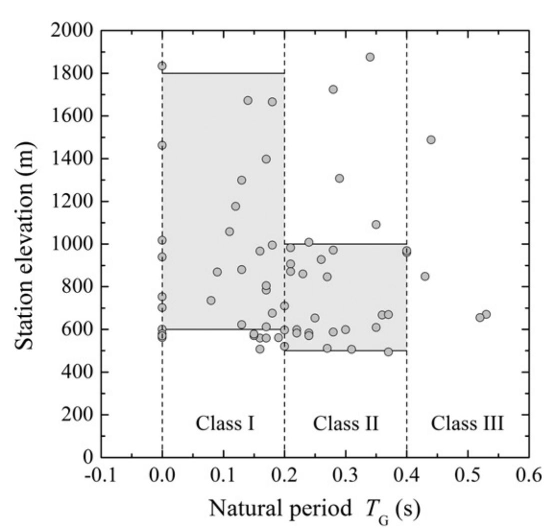

Fig. 16. Station elevation versus its natural period T_G identified by HVSR. Two dashed lines indicate the bounds of two adjacent site classes provided in Table 1. The shaded area means the major elevation interval distribution of Classes I and II, respectively.

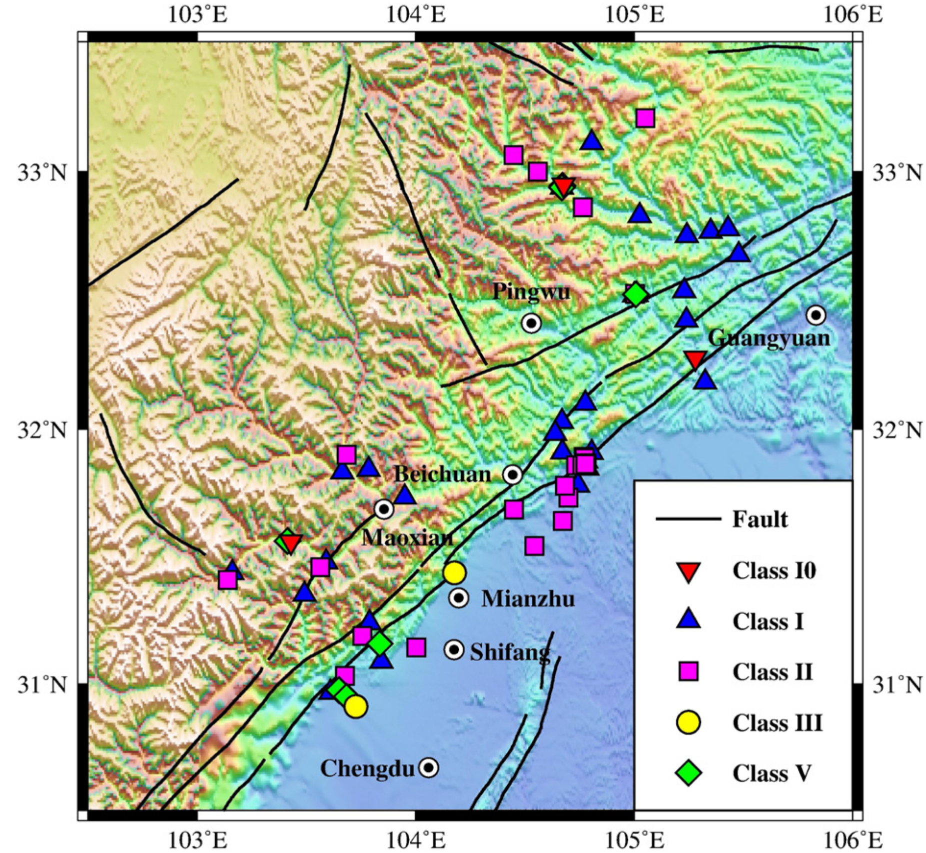

Fig. 17. Recommended site classes for 66 temporary strong-motion stations used in the 2008 Wenchuan earthquake aftershocks.

where d_i is the rank difference between each HVSR value for the ith period with respect to the kth site class, and n is the total number of periods. The SI_k of both Methods 2 and 3 is used for measuring the correlation between the mean HVSR curve for the site of interest without taking the frequency distribution into account. $SI_k = 1$ indicates a perfect positive correlation.

Method 4: Wen et al. (2011) demonstrated that identical contributions to SI for each spectral period sometimes lead to a false classification for Methods 1 and 2, and proposed a weighted HVSR classification method, where the weight of each spectral period is calculated by applying entropy weight theory.

4.2. Proposed classification criterion

For Methods 2, 3 and 4, the standard HVSR shapes of the four classes shown in Fig. 11 were established by Zhao et al. (2006) based on K-NET strong-motion data. Their amplitudes vary considerably for the different spectral periods, but a distinct peak appears for each class curve and could be treated as the natural period. However, in actual field situations the seismic response at any given site is very complicated. The average H/V ratios may either have peaks at several spectral periods, or a flat curve, such as at hard rock sites, and therefore it would be difficult to identify their natural periods.

Therefore, a new scheme of six site classifications is proposed based on Zhao et al. (2006), as listed in Table 3. Classes I, II, III and IV correspond to the match of spectral shape in the four classes of Zhao et al. (2006). However, when the HVSR curve for a site is flat without any evident peaks, it cannot correlate to any spectral ratio shapes and this site should be considered as a separate class. If the HVSR amplitude is close to unity at all spectral periods, it is classified as Class I0, indicating a hard rock site; if larger than unity at all spectral periods, it is classified as Class I, indicating a soft rock site.

As an example of Class I0, Fig. 12(a) shows that station L2003 has a flat average spectral ratio with an average value close to 1 at all spectral periods, a likely hard rock site. Fig. 12(b) shows the spectral ratios from station L2011 as an example of the proposed Class I, because the average HVSR ratios are larger than 1 at all spectral periods.

When the HVSR curve exhibits multiple peaks and the site could arguably correlate to either of the two different classes in Zhao et al.'s (2006) scheme, we assigned Class V to this site. Fig. 13 shows a typical example of Class V site for station L2009, where two predominant periods with identical amplitudes are found visually at 0.14 s and 0.40 s. This spectral shape matches either SC I or SC III of Zhao et al. (2006), and has thus been reclassified as Class V.

4.3. Dataset

To ensure a more stable HVSR curves, the stations selected for site classification must have recorded at least five events and total 66 free-field stations met this requirement, associated with 2451 records. Since the baseline offset of a strong-motion record does not affect the peak ground acceleration, the short- or middle-period acceleration, velocity, or displacement response spectrum (Boore, 2001), the data processing of such records only includes Butterworth filtering for the 0.25–25 Hz bandwidths in the 0.05–3.0 s period range relevant to this study. The 5% damped H/V velocity response spectral ratio was calculated for each record instead of the traditional H/V ratio of the Fourier amplitude spectrum. The geometric mean, H, of the two horizontal components of HSVR for each record is obtained from:

$$\ln(H) = \frac{\ln(\mathrm{EW}) + \ln(\mathrm{NS})}{2} \tag{3}$$

where NS and EW are the north–south and east–west components. The geometric mean and standard deviation of HVSR for all records were calculated for each station.

5. Results and discussion

For Method 1, it was noted that for some stations the peak period was not unique (e.g. for L2009 shown in Figure 13). Table 4 lists 13 stations that have more than one peak period. The spectral period of the larger peak ratio was taken as the natural period T_G (e.g. 0.40 s for L2009 mentioned above, giving Class III by Method 1). In addition, Method 1 classified those stations as Class I whose HVSR peak period was difficult to identify (e.g. L2003 and L2011 in Figure 12).

The proposed Classes I0 and V were assigned first to some stations according to the definition in Table 3 (starred items in Table 4), then the same process were carried by using Methods 2, 3 and 4. The numbers of sites in each site class identified by using each method are listed in Table 5 for all sites. Most fall into either Class I or Class II and no Class IV sites were identified by Methods 1, 2 and 4, consistent with their surface geology in high-altitude, mountainous terrain (mostly in Sichuan Province in China) where the Quaternary soil layer is relatively thin.

The stations classified as Class IV by Method 3 were L0027, L2011, L2012, L2018 and L2025. Most of them were classified as Class I by the other three methods. It is notable that the natural period was either around 0.1 s (e.g. L0027 in Figure 14) or could not be identified by HVSR (e.g. L2011, Figure 12). This reveals the limitation of Method 3, the tail joggle phenomenon defined by Wen et al. (2011) that may lead to a false classification because the HVSR amplitudes at tail periods (>0.6 s) adjacent to Class IV compared with the other three classes of Zhao et al. (2006).

Three hard-rock sites, L0021, L2003 and L2019, were then classified as Class I0 (see Table 4). L0021 site was adjacent to the hydropower plant of Malu Town in Qingchuan County, and the record from this site may be considered to be suitable as a ground-motion input for a dynamic response analysis of the dam. L2003 is one station of the terrain effect array and could be used as the reference site for the analysis of the topography effect on ground motion, since it experienced almost no site response. Two stations, L0008 and L0017 classified as Class III, were located in the plain area (Figure 15) where soft soil deposits may have caused the large observed site amplification in the middle-period range, and the HVSR coincidently matched the Class III criterion of Zhao et al. (2006).

As shown in Appendix A, most stations were located at high elevations. Fig. 16 plots the station elevation vs. natural period T_G identified by HVSR; it appears that these variables are correlated. For stations with flat HVSRs, T_G is difficult to identify and is therefore assumed to be zero. The vertical dashed lines in Fig. 16 show the endpoints of the site classes defined in Table 2. Most Class I sites ($0 < T_G < 0.2$ s) locate at elevations from 600 m to 1800 m, and Class II sites (0.2 s $\leq T_G < 0.4$ s) from 500 m to 1000 m, as indicated by the shaded areas in Fig. 16. It reveals that most of the Class I stations were in mountainous areas, and many Class II stations were in plain areas, matching the actual geological setting.

Method 4 is relatively practical which has been demonstrated by Wen et al. (2011) for some Chinese permanent strong-motion stations so we recommend site classification by the updated Method 4 as shown in Fig. 17, according to the site class definition presented in Table 2 for all stations. Note that none of the stations is in Class IV.

6. Conclusions

Following a brief review of temporary strong-motion observations in China, results from temporary observation for the Wenchuan aftershocks were presented. Site classifications were carried out for some of temporary stations.

(1) Total 3250 records from 949 aftershocks were obtained at 92 temporary stations, and the magnitude, epicentral distance and PGA for each record are presented. The present study shows that the capacity of permanent strong-motion network is obviously inadequate to record near-field ground motions during the 2008 Wenchuan Earthquake sequence, however the temporary observation network can effectively enhance the capacity in capturing near-source records from large aftershocks. For the typical $M_S = 6.0$ earthquake on August 1, 2008, the recorded PGAs from both permanent and temporary networks are compared with the empirical GMPEs for the southwestern China. A large number of strong-motion records were obtained by the temporary observation network and some have higher amplitudes and shorter epicentral distances than the records from the permanent stations for many aftershocks. These records could have a great contribution to studies on the generation, propagation and ground behavior of near-field ground motions.

(2) An updated classification criterion for six site classes is proposed. It is much more practicable than previous schemes. The HVSR technique has been updated for site classification of the temporary stations, and the site classes from 66 stations are recommended. A preliminary analysis of the correlation between station elevation and its natural period T_G identified by HVSR indicates that T_G was generally smaller at higher elevations in Sichuan area. The suggested site class for each station in the present study may be an option for site effect modeling in developing a ground-motion prediction equation (GMPE) based on Chinese dataset. Note that the HVSR of a given site may contain site effect (for example, minor or moderate topography effect), that is not consistent with the code site class which is usually based on the surface soil shear-wave velocity profile and bedrock depth. Therefore, further checks on the site class derived in the present study should be carried out using more specific surface setting, geotechnical data and field investigations if possible.

The temporary strong-motion observation stations for gathering strong-motion records for the 2008 Wenchuan earthquake sequence is a successful case, and it is highly effective for collecting near-field strong-motion records from aftershocks, to compensate the sparse distribution of the permanent stations in China, at least at the present time.

7. Data source

All the strong-motion data used in this paper could be applied from China Strong-motion Networks Center (www.csmnc.net).

Acknowledgments

This work is supported by the National Natural Science Fund Nos. 51308515 and 51278473, and Nonprofit Industry Research Project of CEA under Grant No. 201108003. We thank the China Earthquake Administration, Sichuan Provincial Earthquake Administration, Yunnan Provincial Earthquake Administration, Gansu Provincial Earthquake Administration, and Hubei Provincial Earthquake Administration for making this operation successful. We thank J. X. Zhao and two anonymous reviewers for their valuable suggestions and constructive comments, which helped us to improve the manuscript. Dr. Yan-Guo Zhou, managing guest editor is appreciated for his help to prepare this paper.

Appendix A. List of temporary strong-motion observation stations

No.	Station code	Station name	Elevation (m)	Longitude (°)	Latitude (°)	Site condition	Starting date	Numbers of recordings				Remarks
								a[1]	b[2]	c[3]	d[4]	
1	L0001	Linjiaba gas station	784	104.67	32.03	Rock	2008/5/21	64	29	9		
2	L0002	Guixi Town	653	104.64	31.98	Rock	2008/5/21	70	17	8		
3	L0003	Hexi gas station	506	104.70	31.73	Soil	2008/5/15	27	1			
4	L0004	Jiangyou City	507	104.74	31.78	Rock	2008/5/15	45	3			
5	L0005	Rangshui gas station	511	104.68	31.78	Soil	2008/5/15	41	5			
6	L0006	Jiuling gas station	494	104.67	31.64	Soil	2008/5/15	15				Due to warning of overflow of the quake lake, the instrument was transferred to L0019 on May 23, 2008
7	L0007	Danjingshan toll station	805	103.84	31.09	Rock	2008/5/16	40	3			
8	L0008	Hanwang gas station	667	104.18	31.44	Soil	2008/5/16	53	9	6		
9	L0009	Yong'an gas station	599	104.45	31.69	Soil	2008/5/16	69	20	3		
10	L0010	Huagai gas station	520	104.54	31.54	Soil	2008/5/16	12				Following earthquake short-term prediction, the instrument was transferred to L0024 on May 31, 2008
11	L0011	CEA emergency response office in Puyang Town	676	103.68	31.03	Soil	2008/5/18	38	12	1		
12	L0012	Yutang Town	710	103.61	30.97	Rock	2008/5/18	5		1		Following earthquake short-term prediction, the instrument was transferred to L0023 on May 30, 2008
13	L0013	Xiaoyudong Town	983	103.76	31.19	Soil	2008/5/20	72	49	21		
14	L0014	Tongji Town	848	103.84	31.16	Soil	2008/5/20	65	17	5		
15	L0015	Xinxing Town	791	103.85	31.13	Rock	2008/5/20					
16	L0016	Gymnasium of Dujiangyan City	670	103.65	30.98	Soil	2008/5/14	12	2		13	Due to retreating of CEA emergency response office, the instrument was transferred to L1007 on June 4, 2008
17	L0017	Chongyi toll station	655	103.73	30.91	Soil	2008/5/14	14	1	1		Following earthquake short-term prediction, the instrument was transferred to L0001 on May 21, 2008
18	L0018	Juyuan toll station	669	103.68	30.95	Soil	2008/5/14	16	2			Following earthquake short-term prediction, the instrument was transferred to L0014 on May 20, 2008
19	L0019	Dakang gas station	599	104.74	31.86	Soil	2008/5/23	12	1			
20	L0020	Dayuan Town	753	105.24	32.43	Rock	2008/5/30	43	23	4	10	
21	L0021	Hydropower plant of Malu Town in Qingchuan County	600	105.28	32.28	Rock	2008/5/30	14	1	2	3	
22	L0022	Jinshan village of Jinshanzi Town	622	105.33	32.18	Rock	2008/5/30	8				
23	L0023	Baoshan corporation of Longmenshan Town	1018	103.79	31.24	Rock	2008/5/30	13	9	2	1	
24	L0024	Huangtu Town, An'xian County	526	104.47	31.59	Soil	2008/5/31	3			1	
25	L0025	Hongyan Town	587	104.00	31.15	Soil	2008/5/16	10				Following earthquake short-term prediction, the instrument was transferred to L0013 on May 20, 2008
26	L0026	Pengzhou City	572	103.95	30.96	Soil	2008/5/16	3				Following earthquake short-term prediction, the instrument was transferred to L0002 on May 20, 2008
27	L0027	Huangping Town	735	105.23	32.54	Rock	2008/8/8	58		108		
28	L0028	Xiangyan Town	612	104.78	32.10	Rock	2008/8/8	9				
29	L0029	Tongkou Town	561	104.58	31.79	Soil	2008/8/2	3				
30	L0030	Communication building of Dujiangyan City, basement	670	103.65	30.99	Structure	2008/6/8	11	3			Building structure array in Dujiangyan City
31	L0031	Communication building of Dujiangyan City, ground floor	670	103.65	30.99	Structure	2008/5/28	20	4	1		Building structure array in Dujiangyan City
32	L0032	Communication building of Dujiangyan City, fourth floor	670	103.65	30.99	Structure	2008/5/28	7	1	1		Building structure array in Dujiangyan City
33	L0033	Communication building of Dujiangyan City, eighth floor	670	103.65	30.99	Structure	2008/5/28	11	2			Building structure array in Dujiangyan City
34	L0034	Shanghai Lane of Jiangyou City, center of ground floor	583	104.73	31.77	Structure	2008/8/13	1				Building structure array in Jiangyou City
35	L0035	Shanghai lane of Jiangyou City, north of ground floor	583	104.73	31.77	Structure	2008/8/13					Building structure array in Jiangyou City
36	L0036	Shanghai lane of Jiangyou City, center of seventh floor	583	104.73	31.77	Structure	2008/8/13	1				Building structure array in Jiangyou City
37	L0037	Shanghai lane of Jiangyou City, north of seventh floor	583	104.73	31.77	Structure	2008/8/13					Building structure array in Jiangyou City
38	L0038	Shanghai lane of Jiangyou City, center of eleventh floor	583	104.73	31.77	Structure	2008/8/13					Building structure array in Jiangyou City
39	L0039	Shanghai lane of Jiangyou City, center of fifteenth floor	583	104.73	31.77	Structure	2008/8/13					Building structure array in Jiangyou City
40	L0040	Shanghai lane of Jiangyou City, north of fifteenth floor	583	104.73	31.77	Structure	2008/8/13	1				Building structure array in Jiangyou City

Appendix A (*continued*)

No.	Station code	Station name	Elevation (m)	Longitude (°)	Latitude (°)	Site condition	Starting date	Numbers of recordings				Remarks
								a[1]	b[2]	c[3]	d[4]	
41	L0041	Douchui Hill 1#	1058	104.81	31.91	Rock	2008/6/25	8	1			Terrain effect array, top of the hill
42	L0042	Douchui Hill 2#	995	104.67	31.91	Rock	2008/6/25	9	1			Terrain effect array, foot of the hill
43	L0043	The forth Panchang steelmaking plant	609	104.77	31.89	Soil	2008/6/25	14	1			Basin effect array in Wudu Town
44	L0044	Taibai middle school, Jiangyou City	597	104.77	31.89	Soil	2008/6/25	11	1	1		Basin effect array in Wudu Town
45	L0045	Group 3 of Xiping village	583	104.78	31.88	Rock	2008/6/25	35	2			Basin effect array in Wudu Town
46	L0046	Group 1 of Dahe village	583	104.78	31.87	Soil	2008/6/25	15	1			Basin effect array in Wudu Town
47	L0047	Group 6 of Nanta village	559	104.79	31.85	Rock	2008/6/25	7				Basin effect array in Wudu Town
48	L0048	Group 3 of Dahe village	559	104.78	31.86	Soil	2008/6/25	34	2			Basin effect array in Wudu Town
49	L0049	Group 4 of Dahe village	561	104.78	31.86	Soil	2008/6/25	24	1			Basin effect array in Wudu Town
50	L0050	Group 8 of Shuangnian village	570	104.76	31.86	Soil	2008/8/10	5				Basin effect array in Wudu Town
51	L0051	Wutong village	570	104.78	31.86	Soil	2008/8/10	5				Basin effect array in Wudu Town
52	L0052	Guanyin Hill 1#	880	105.00	32.52	Rock	2008/8/14	26		12		Terrain effect array, foot of the hill
53	L0053	Guanyin Hill 2#	967	105.00	32.52	Rock	2008/8/14	20		4		Terrain effect array, top of the hill
54	L0054	Sanguo Town	907	105.01	32.53	Soil	2008/8/14	13		4		Basin effect array in Sanguo Town
55	L0055	Group 4 of Dongyang village	871	105.00	32.53	Soil	2008/8/14	21		6		Basin effect array in Sanguo Town
56	L0056	Group 8 of Dongyang village	869	105.01	32.52	Rock	2008/8/14	12		2		Basin effect array in Sanguo Town
57	L1001	Huilong hydrological station, Maoxian County	1672	103.66	31.83	Rock	2008/6/3	10	2			
58	L1002	Shidaguan Town, Maoxian County	1724	103.68	31.90	Soil	2008/6/3	8				
59	L1003	Seergu gas station, Heishui County	1811	103.42	31.94	Rock	2008/6/3	2				
60	L1004	Huilong Town, Maoxian County	1666	103.79	31.84	Rock	2008/6/3	25	45	6		
61	L1005	Goukou Town, Maoxian County	1614	103.78	31.78	Rock	2008/6/3	2				
62	L1006	Feihong Town, Maoxian County	1643	103.73	31.80	Soil	2008/6/3					
63	L1007	Earthquake Bureau of Dujiangyan City	682	103.61	31.00	Soil	2008/6/4				14	
64	L1008	Fuli gas station, Wenchuan County	1110	103.61	31.49	Rock	2008/5/24				32	
65	L1009	Xiaolong Primary school in Nanchong City	297	106.15	30.84	Rock	2008/5/26					
66	L2001	Zhongmiao Town	578	105.35	32.77	Rock	2008/5/23	105	79	53		
67	L2002	Wenxian seismological station 1#	960	104.67	32.95	Soil	2008/5/17	59	4			Terrain effect array, middle of the hill
68	L2003	Wenxian seismological station 2#	940	104.68	32.95	Rock	2008/5/17	15	2	2		Terrain effect array, middle of the hill, in a cave
69	L2004	Shifang Town	972	104.56	33.00	Soil	2008/5/23	20				
70	L2005	Danbao Town	860	104.77	32.86	Soil	2008/5/24	47	1			
71	L2006	Bikou hydropower plant	579	105.24	32.75	Rock	2008/5/23	99	59	40		
72	L2007	Wenxian seismological station 3#	927	104.67	32.94	Rock	2008/5/17	43	2			Terrain effect array, foot of the hill
73	L2008	Shijiba Town	1091	104.45	33.06	Soil	2008/5/23	25				
74	L2009	Wenxian seismological station 4#	969	104.67	32.94	Soil	2008/5/17	88	11	2		Terrain effect array, top of the hill
75	L2010	Yulei Town	702	105.03	32.83	Rock	2008/5/24	39	7	2		
76	L2011	Shazhou Town, Qingchuan County	562	105.48	32.68	Rock	2008/5/28	37	13	14		
77	L2012	Yaodu Town, Qingchuan County	569	105.43	32.78	Rock	2008/5/28	52	12	70		
78	L2013	Dam of Bikou Hydropower plant 1#	586	105.23	32.76	Structure	2008/5/28	84	28	9		Dam structure array in Jiangyou City, foot of the dam
79	L2014	Dam of Bikou Hydropower plant 2#	676	105.23	32.76	Structure	2008/5/28	78	16	3		Dam structure array in Jiangyou City, top of the dam
80	L2015	Waina Town	846	105.05	33.21	Soil	2008/5/21	35				
81	L2016	Qiaotou Town	1008	104.81	33.11	Rock	2008/5/21	26		4		
82	L2017	Putou Town, Lixian County	1876	103.14	31.41	Soil	2008/5/14	11	6	2		
83	L2018	Earthquake bureau of Lixian County	1834	103.16	31.44	Rock	2008/5/15	18	2	2		
84	L2019	Tonghua gas station, Lixian County	1463	103.43	31.56	Rock	2008/5/14	7	1			
85	L2020	Tonghua Town, Lixian County	1488	103.41	31.56	Soil	2008/6/18	26	1	3		
86	L2021	CEA emergency response office in Wenchuan County	1298	103.58	31.48	Soil	2008/5/18	3				
87	L2022	Wenchuan seismological station	1299	103.59	31.48	Rock	2008/5/16	8	2	1		
88	L2023	Yanmenguan, Wenchuan County	1339	103.61	31.49	Soil	2008/5/18	1				
89	L2024	Mianchi Town, Wenchuan County	1198	103.49	31.36	Soil	2008/5/17	2	1			
90	L2025	Qiangfeng gas station, Wenchuan County	1177	103.49	31.35	rock	2008/5/18	52	4	18		
91	L2026	Guozhupu, Wenchuan County	1307	103.56	31.46	Soil	2008/5/18	16				
92	L2027	Guangming Town, Wenchuan County	1398	103.95	31.74	Rock	2008/6/18	26	3	4		
			Total					2214	525	437	74	

Note:

[1]Records have been published and described in the official earthquake catalog of the China Earthquake Network Center (CENC).

[2]Records have been published and are likely to be associated with a given event in the earthquake catalog produced by the regional Sichuan Province seismic network.

[3]Records have not been published and cannot be related to any events in either of the two earthquake catalogs.

[4]Records have not been published and their exact record times were automatically reset by the accelerograph due to power outages.

References

Boore, D.M., 2001. Effect of baseline corrections on displacements and response spectra for several recordings of the 1999 Chi-Chi, Taiwan. Bull. Seismol. Soc. Am. 91 (5), 1199–1211.

Building Seismic Safety Council (BSSC), 2003. The 2003 NEHRP recommended provisions for new buildings and other structures. Part I (Provisions) and Part II (Commentary), FEMA 368/369, Washington, D.C.

China Earthquake Administration, 2006. Specification for the construction of seismic station, strong-motion station (DB/T-2006) (in Chinese).

Gao, G., Yu, H., Li, S., 2001. Strong ground motion observation for China mainland. World Earthq. Eng. 17 (4), 13–18 (in Chinese).

Ghasemi, H., Zare, M., Fukushima, Y., Sinaeian, F., 2009. Applying empirical methods in site classification, using response spectral ratio (H/V): a case study on Iranian Strong Motion Network (ISMN). Soil Dyn. Earthq. Eng. 29 (1), 121–132.

Huo, J.R., 1989. Study on the attenuation laws of strong earthquake ground motion near the source. Ph.D. Dissertation , Institute of Engineering Mechanics, China Earthquake Administration.

Japan Road Association, 1980. Specifications for Highway Bridges, Part V, Seismic Design. Maruzen Co., LTD., Tokyo.

Li, X.J., 2009a. Report on Strong Earthquake Motion Records in China, 13(1), Uncorrected Acceleration Records from Permanent Observation for Wenchuan MS8.0 Aftershocks. Seismological Publishing House, Beijing (in Chinese).

Li, X.J., 2009b. Report on Strong Earthquake Motion Records in China, 14(1), Uncorrected Acceleration Records From Temporary Observation for Wenchuan MS8.0 Aftershocks. Seismological Publishing House, Beijing (in Chinese).

Li, X.J., Zhou, Z.H., Yu, H.Y., Wen, R.Z., Lu, D.W., Huang, M., Zhou, Y.N., Cu, J.W., 2008. Strong motion observations and recordings from the great Wenchuan Earthquake. Earthq. Eng. Eng. Vib. 7 (3), 235–246.

Liu, H.X., 1986. The Damages of the Great Tangshan Earthquake, Volume I. Seismological Publishing House, Beijing (in Chinese).

Wen, R.Z., Zhou, Z.H., Li, X.J., 2009. The strong ground motion observation for the Wenchuan aftershock. Earthq. Sci. 22 (2), 181–187.

Wen, R.Z., Ren, Y.F., Zhou, Z.H., Shi, D.C., 2010. Preliminary site classification of free-field strong motion stations based on Wenchuan earthquake records. Earthq. Sci. 23 (1), 101–110.

Wen, R.Z., Ren, Y.F., Shi, D.C., 2011. Improved HVSR site classification method for free-field strong motion stations validated with Wenchuan aftershock recordings. Earthq. Eng. Eng. Vib. 10 (3), 325–337.

Zhao, Y.Q., Cui, J.W., Qiao, S., Bao, Y.F., Lu, J.G., Fu, Z.X., Yang, K.J., 2001. The strong earthquake observation records of the Shidian Earthquake and their preliminary analysis. J. Seismol. Res. 24 (3), 245–250 (in Chinese).

Zhao, J.X., Irikura, K., Zhang, J., Fukushima, Y., Somerville, P.G., Asano, A., Ohno, Y., Oouchi, T., Takahashi, T., Ogawa, H., 2006. An empirical site-classification method for strong-motion stations in Japan using H/V response ratio. Bull. Seismol. Soc. Am. 96 (3), 914–925.